Genomics Proteomics Bioinformatics 11 (2013) 230–240

Genomics Proteomics Bioinformatics

www.elsevier.com/locate/gpb
www.sciencedirect.com

ORIGINAL RESEARCH

Quantitative Evaluation of Aldo–keto Reductase Expression in Hepatocellular Carcinoma (HCC) Cell Lines

Lei Yang [1], Ju Zhang [1], Shenyan Zhang [1], Weiwei Dong [2], Xiaomin Lou [1], Siqi Liu [1,*]

[1] *CAS Key Laboratory of Genome Sciences and Information, Beijing Institute of Genomics, Chinese Academy of Sciences, Beijing 100101, China*
[2] *Department of Oncology, General Hospital of PLA, Beijing 100853, China*

Received 27 March 2013; revised 31 March 2013; accepted 7 April 2013
Available online 11 April 2013

KEYWORDS

Aldo–keto reductase;
HCC;
Quantitative analysis;
Real-time PCR;
Multiple reaction monitoring

Abstract The involvement of aldo–keto reductases (AKRs) in tumorigenesis is widely reported, but their roles in the pathological process are not generally recognized due to inconsistent measurements of their expression. To overcome this problem, we simultaneously employed real-time PCR to examine gene expression and multiple reaction monitoring (MRM) of mass spectrometry (MS) to examine the protein expression of AKRs in five different hepatic cell lines. These include one relatively normal hepatic cell line, L-02, and four hepatocellular carcinoma (HCC) cell lines, HepG2, HuH7, BEL7402 and SMMC7721. The results of real-time PCR showed that expression of genes encoding the AKR1C family members rather than AKR1A and AKR1B was associated with tumor, and most of genes encoding AKRs were highly expressed in HuH7. Similar observations were obtained through MRM. Different from HuH7, the protein abundance of AKR1A and AKR1B was relatively consistent among the other four hepatic cell lines, while protein expression of AKR1C varied significantly compared to L-02. Therefore, we conclude that the abundant distribution of AKR1C proteins is likely to be associated with liver tumorigenesis, and the AKR expression status in HuH7 is completely different from other liver cancer cell lines. This study, for the first time, provided both overall and quantitative information regarding the expression of AKRs at both mRNA and protein levels in hepatic cell lines. Our observations put the previous use of AKRs as a biomarker into question since it is only consistent with our data from HuH7. Furthermore, the data presented herein demonstrated that quantitative evaluation and comparisons within a protein family at both mRNA and protein levels were feasible using current techniques.

Introduction

Aldo–keto reductases (AKRs), which include approximately 160 members, are a protein superfamily that is widely distributed from prokaryotes to eukaryotes [1–3]. Most AKRs are generally believed to be the pivotal enzymes for the detoxification of reactive aldehydes [4]. To date, 13 AKR proteins have been identified in humans, including AKR1A1 (aldehyde

* Corresponding author.
E-mail: siqiliu@big.ac.cn (Liu S).

Peer review under responsibility of Beijing Institute of Genomics, Chinese Academy of Sciences and Genetics Society of China.

ELSEVIER Production and hosting by Elsevier

http://dx.doi.org/10.1016/j.gpb.2013.04.001

reductase), AKR1B1 and AKR1B10 (aldose reductase), AKR1C1–1C4 (hydroxysteroid dehydrogenase, HSD), AKR1D1 (Δ4-3-ketosteroid-5β-reductase), AKR6A3, AKR6A5, AKR6A9 (Kvβ), AKR7A2 and AKR7A3 (aflatoxin aldehyde reductase) [4,5]. Over recent years, it has become increasingly clear that many human AKRs are intimately linked with cancer biology. Expression of some AKR1 members that may be induced by oxidative stress and participate in different signaling pathways of cell proliferation was increased in different types of cancer. For example, expression of AKR1B10 and AKR1C3 increased the risk of cancer in the target organ through the retinal reductase activity, thus leading to reduction in retinoic acid (RA) biosynthesis [6]. AKR7 family is involved in the metabolism of aflatoxin [7], which is a well-known carcinogen for the liver. Despite these studies, the significance of the involvement of AKRs in cancers, however, is not yet fully elucidated. Moreover, which AKR member is specifically related with cancer type is still inconclusive. For instance, overexpression of AKR1B10 was considered as a novel biomarker for non-small cell lung carcinoma (NSCLC) [8]. The association of AKR1B10 in NSCLC with smoking was established by microarray analysis and confirmed by RT-PCR, immunobloting and immunohistochemistry (IHC) in paired samples of squamous cell carcinomas (SCC) and noncancerous tissues [8–11]. However, the association did not gain strong support from other large screenings in genomics, transcriptomics, and proteomics [12]. Lin et al. reported that, AKR1C3 was consistently overexpressed in ductal carcinoma tissues of breast cancer *in situ* using IHC [13]. Ji et al. took a similar strategy but came to the opposite results that selective loss of AKR1C1 and AKR1C2 was found in 24 paired breast cancer tissues, whereas AKR1C3 was only minimally affected in the same samples [14]. Besides AKR1B10 and AKR1C3, abnormal expression of other AKR members, such as AKR1A1 [15], AKR1B1 [16,17], AKR1C1, AKR1C2 and AKR1C4 [14,18–29], was detected in various cancer tissues or cells. However, employment of different approaches in different studies has led to conflicting results, which are not easily further cross validated by other approaches or laboratories due to the different samples examined, expression levels and even different cut-offs.

The controversial observations regarding AKRs and cancer necessitate the development of an approach to accurately evaluate the AKR abundances in cells and tissues. Fundamentally, three questions ought to be addressed. First of all, most previous studies on AKR gene expression have only reported one or several AKR members, there lacks general understanding of the expression profile for all the AKR family members. As many AKR enzymes convert the similar substrates following the same catalytic mechanism *in vivo* [30], it is likely that the protein abundances would compensate for each other [31,32]. Therefore, focusing on individual AKRs rather than the family has probably led to misinterpretation of the biological significance of the expression status of AKRs in cancers. Secondly, the conflicting conclusions regarding AKR expression were often drawn from different measurements, at mRNA or protein level. As mRNA abundance is not closely and linearly correlated with protein abundance for many genes, conclusion only derived from the mRNA or protein assay may lead to a distorted view of expression. Hence, monitoring the AKR expression status in cells or tissues at both mRNA and protein levels should be more appropriate. Thirdly, for global screening of the tumor-associated genes, traditional techniques such as DNA/RNA array and protein profiling are often lacking in accurate quantitative information, such that screening data are not always comparable with targeting data in biomarker discovery. How to quantitatively evaluate the AKR expression is another key issue required to clarify the controversial argument of the relationship of AKRs with cancers. Therefore, we carried out the global evaluation of the AKR expression status in cancer cell lines, trying to address the three issues mentioned above.

Liver is an important organ involved in detoxification in the human body and contains all types of human AKR proteins to perform such functions. Several investigators reported that the abnormal expression of AKR proteins in liver tumor tissues or cells possibly resulted in loss of detoxification functions [33,34]. For instance, Cao et al. observed that expression of AKR1A1 remained unchanged while AKR1B1 was overexpressed in HCC [35]. However, Goh et al. found that expression of AKR1A1 was decreased, while AKR1B1 did not change significantly in HCC [36]. Therefore, liver cancer cells or tissues would be ideal for quantitatively evaluating the AKR expression status, either to detect the expression of AKR members globally or to clarify the argument on the AKR roles in liver cancers. Therefore, four liver cancer cell lines were chosen to evaluate the global expression of AKRs. The obtained results were further validated at the protein level using 55 pairs of HCC samples and adjacent tissues.

In this study, we designed an analysis strategy aiming at globally and quantitatively to determine the abundance of individual AKRs at both mRNA and protein in the selected cell lines. We employed real-time PCR to monitor the expression of AKR mRNAs and MRM-based MS to detect the expression of AKR proteins. With calibration and normalization, we produced the profiles for the abundance distribution of all the AKR gene products, and demonstrated the correlation of the AKRs and cancer cell lines.

Results

Preparation for quantitative evaluation of AKR expression in hepatic cell lines and tissues

Totally 13 AKRs have been reported in human. These include 10 AKRs with the aldo–keto enzyme activities, such as AKR1A1, AKR1B1, AKR1B10, AKR1C1–1C4, AKR1D1, AKR7A2 and AKR7A3, and 3 AKRs without the catalytic functions, such as AKR6A3, AKR6A5 and AKR6A9. As detoxification by AKRs is believed to be involved in tumorigenesis and tumor development, the AKR members without enzymatic activities were not considered in this study. Besides, there is a high homology in the amino acid sequences of AKR1C1 and AKR1C2 (approximately 97%) and the high identity of the two genes makes the measurement at either mRNA or protein levels technically difficult. These two AKRs were thus regarded as a single protein product termed as AKR1C1/1C2 in this study. In total, 9 AKRs were selected for quantitative evaluation of their expression, including AKR1A1, AKR1B1, AKR1B10, AKR1C1/1C2, AKR1C3, AKR1C4, AKR1D1, AKR7A2 and AKR7A3. Each unique peptide had four qualified transitions.

The techniques of real-time PCR and MRM are appropriate for the quantification of mRNA and protein abundances, because they can provide relatively accurate quantitative information. During measurements, design of both the real-time PCR primers and the MRM unique peptides for each AKR is fundamentally important to clearly distinguish the AKR members. As a matter of fact, it was not an easy job to select the primers or peptides in such enzyme family, since these members share such high sequence homology at either nucleotide or amino acid levels. Primers that are able to amplify the unique sequences of various AKR genes with a length of 100–200 bp were synthesized and carefully evaluated for amplification in pilot experiments prior to the real-time PCR experiments (sequencing validation was shown in Figure S1). However, expression of AKR1D1 and AKR7A3 was not detected in our samples (data not shown). In peptide design for MRM, the similar difficulty appeared in selecting multiple unique peptides of AKRs due to the highly homologous amino acid sequences in AKR proteins. Thus the selection of proper peptides/transitions was based on the recombinant AKRs identified by MS. Using data-independent acquisition to detect all the digested peptides of each AKR protein in an EMS–EPI scan (the shotgun scan preformed on QTRAP5500 by a combination of enhanced MS and product ion scans), high quality MS/MS signals corresponding to the AKR peptides were acquired. Furthermore, according to the criteria for selecting the MRM peptide, the AKR transitions were predicted with MRM pilot in MRM–EPI mode (MRM triggered enhanced product ion scan). Taking into accounts of the scanning results from EMS–EPI and MRM–EPI upon the AKR recombinant peptides, numbers of qualified AKR peptides for MRM were finally defined, that is, two unique peptides for AKR1A1, AKR1B1 and AKR1B10, and single unique peptide for the remaining AKR1C1/1C2, AKR1C3, AKR1C4 and AKR7A2.

According to our experimental design, it would be valuable to evaluate the AKR expression not only within cell lines but also at tissue level. Technically speaking, both techniques, real-time PCR and MRM, are difficult to use in tissue samples, whereas IHC is a proper approach to detect the AKRs if the AKR antibodies are available. Unfortunately, appropriate antibodies for IHC against the 7 AKRs are not yet commercially available. So we developed the specific monoclonal antibodies against AKRs by using the full length or truncated recombinant AKRs as the antigens (Figure S2). Appropriate monoclonal AKR antibodies were characterized based upon two criteria: 1) no cross reactions between any AKR recombinant proteins, and 2) single band appeared in Western blot against the cell lysate (Figure S2).

Quantitative AKR transcriptomes in hepatic cell lines

In all the hepatic cell lines, strong signals were detected for AKR mRNAs using real-time PCR with actin as the internal control in triplicate experiments, although the signal was relatively lower in L-02 for AKR1C4. **Figure 1** shows the relative transcript abundance of AKRs in each hepatic cell line. It is readily noticed that the mRNA abundance of almost AKR members in HuH7 was dramatically higher than that in the other hepatic cell lines. In human genome, AKR1A1 and AKR7A2 are located on chromosome (Chr) 1p, AKR1B1 and AKR1B10 are found on Chr 7q, while all the AKR1Cs are located on Chr10p. The globally higher AKR transcription in HuH7 thus implies that there may occur abnormality in copy numbers of chromosomes in HuH7 cells (see characterization of HuH7 in JCRB cell bank), at least for Chr 1, 7 and 10 where AKR genes are located. Of the four hepatic cancer cell lines examined in this study, only HuH7 exhibited the unique features of AKR mRNA abundance. Therefore, we suspect that whether AKR expression in HuH7 is representative for hepatic cancer is thus questionable in the field. The mRNA abundant profiles presented in Figure 1 indeed contained plentiful information regarding AKR expression status. Except for HuH7, mRNA abundance for four AKRs remained relatively stable both in normal and tumor cell lines, following

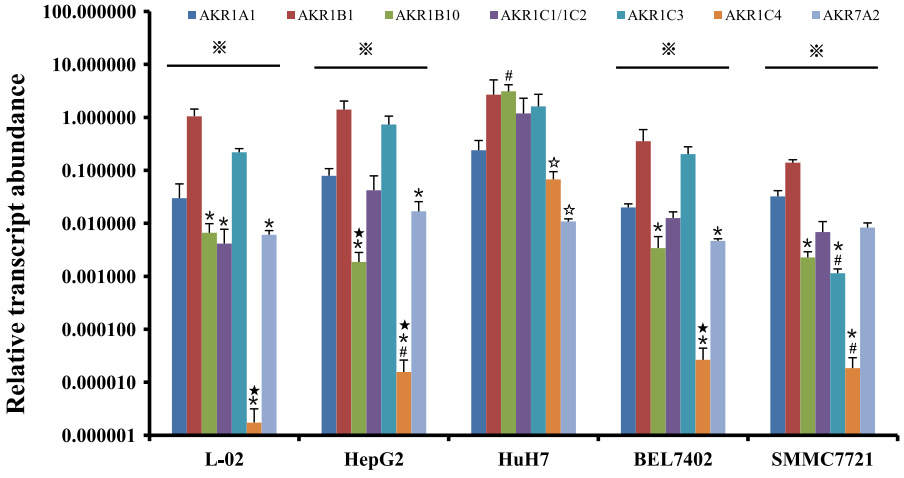

Figure 1 Relative mRNA abundance of each AKR in hepatic cell lines by real-time PCR

Relative mRNA abundance of each AKR was measured by real-time PCR in 5 hepatic cell lines, respectively (one relative normal cell line L-02, with four HCC cell lines HepG2, HuH7, BEL7402 and SMMC7721). The △Ct values of AKRs were normalized by those of housekeeping gene ACTB in respective cell lines. The comparison of mRNA abundances of the AKRs was achieved by $2^{-\triangle\triangle Ct}$ method. Significant differences in abundance are denoted with #, *, ☆ and ★, when compared to AKR1A1, AKR1B1, AKR1B10 and AKR1C3, respectively. ※ indicates significant difference between respective cell lines and HuH7. $n = 5$; $P < 0.05$.

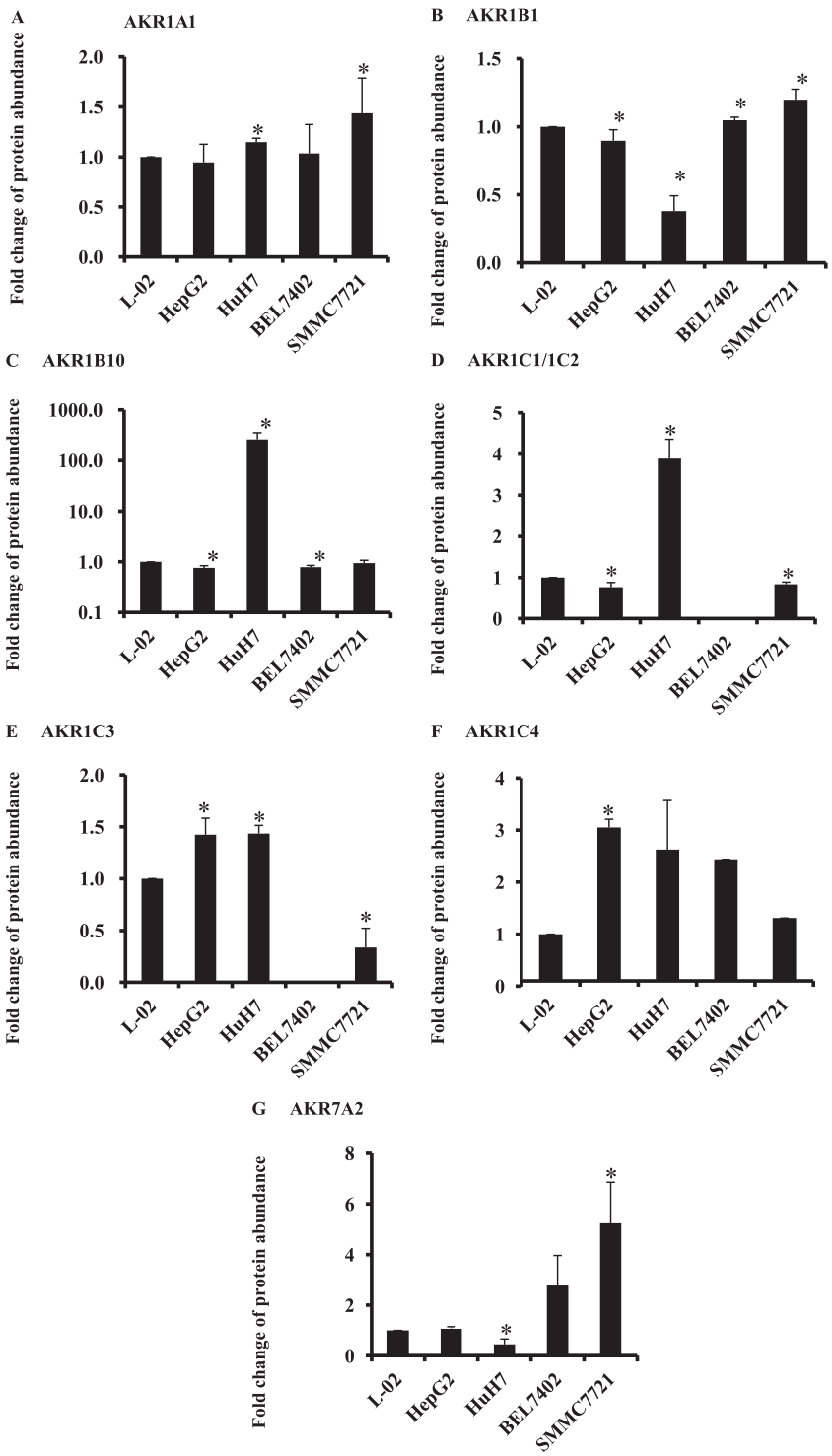

Figure 2 Relative protein abundance of each AKR in hepatic cell lines

Relative protein abundance of each AKR was measured by MRM in 5 hepatic cell lines, respectively (one relative normal cell line L-02, with four HCC cell lines HepG2, HuH7, BEL7402 and SMMC7721). The fold changes of AKR1A1 (**A**), AKR1B1(**B**), AKR1B10 (**C**), AKR1C1/1C2 (**D**), AKR1C3 (**E**), AKR1C4 (**F**) and AKR7A2 (**G**) protein in four HCC cell lines were calculated, with changes in L-02 set as 1. $n = 4$ (except $n = 1$ for AKR1C4 in BEL7402 and SMMC7721); *indicates significant difference compared to L-02 ($P < 0.05$).

the abundance order as AKR1B1 > AKR1A1 > AKR7A2 > AKR1B10. Therefore, mRNA abundance distribution patterns for theses four AKRs in these cell lines are unlikely to bear any cancer characteristics. However, the mRNA abundance distribution of AKR1C displayed different patterns within the cell lines. mRNA abundance of AKR1C1/1C2 was lower than that of AKR1C3 in L-02, HepG2 and BEL7402, while the relative mRNA abundance ratio of

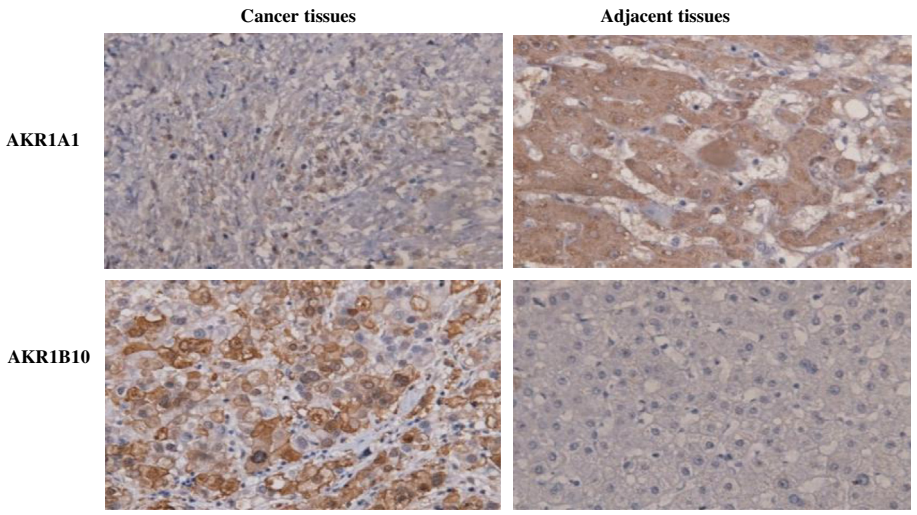

Figure 3 Distribution of AKR1A1 and AKR1B10 protein in HCC

Totally, 55 pairs of HCC and their adjacent tissues were examined. Shown here are representative images for AKR1A1 (upper panel) and AKR1B10 (lower panel). Staining intensity of AKR1B10 in cancer regions was relative higher than that in adjacent tissues, whereas AKR1A1 exhibited the opposite trends. All images were taken with 400× magnification.

AKR1C1/1C2 to AKR1C3 in SMMC7721 was in the opposite direction. Moreover, mRNA abundance of AKR1C4 in all the tumor cell lines was significantly higher than that in L-02. Taking all together, the transcriptional status of the AKR1C family members rather than that of AKR1A and AKR1B may have tumor-related significance. It is interesting to note that mRNA expression of AKR1B10 was remarkably high in HuH7 (more than 400 folds than that in L-02, $P < 0.05$), even higher than that of AKR1B1. AKR1B1 and AKR1B10 are located on Chr 7q35 and 7q33, respectively. Whether the extremely abnormal expression of AKR1B10 could be associated with the chromosomal position during tumorigenesis remains to be further explored.

Quantitative AKR proteomes in hepatic cell lines

In most cells, the selected AKR peptides with the corresponding transitions generated high quality MRM signals, which were satisfactory for accurate quantification based upon the mass differential tags for relative and absolute quantification (mTRAQ) approach. The corresponding peptide signals were easily detected in L-02, HepG2 and SMMC7721 (Table S1). However, we failed to acquire MRM signals of AKR1C1/1C2 and AKR1C3 in BEL7402 for unknown reasons, although mRNA abundance of AKR1C1/1C2 and AKR1C3 in BEL7402 was comparable to that in the other three cell lines. Therefore, we suspect that some interference in the m/z range of the AKR1C1/1C2 and AKR1C3 peptides in BEL7402 may block the generation of the corresponding transitions. Compared to the other cell lines, HuH7 still showed quite distinct features in AKR abundance. In particular, the abundance for AK1B10 and AKR1C1/1C2 was increased significantly compared to L-02 ($P < 0.05$), while that in the other cell lines was decreased or remained unchanged. The protein abundance of the other AKRs in HuH7, however, showed different patterns from the abundance of their corresponding mRNAs. Abundance of AKR mRNAs in HuH7 were globally higher than that in the other cell lines (Figure 1), whereas abundance of AKR1A1, AKR1B1 and AKR7A2 proteins in HuH7 had no significant increase (**Figure 2**). In these cells, what kind of changes in translation or protein degradation might be responsible for AKR abundances remains a

Table 1 IHC results of human AKR monoclonal antibodies

AKR	Tissue samples	Total No.	Negative No. (%)	Positive No. (%)	*P* value
AKR1A1	Cancer tissues	55	37 (67.27%)	18 (32.73%)	0.007
	Adjacent tissues	55	23 (41.82%)	32 (58.18%)	
AKR1B10	Cancer tissues	55	18 (32.73%)	37 (67.27%)	0.007
	Adjacent tissues	55	32 (58.18%)	23 (41.82%)	
AKR1C1/1C2	Cancer tissues	55	36 (65.45%)	19 (34.55%)	1.000
	Adjacent tissues	55	36 (65.45%)	19 (34.55%)	
AKR1C3	Cancer tissues	55	22 (40.00%)	33 (60.00%)	0.846
	Adjacent tissues	55	23 (41.82%)	32 (58.18%)	
AKR1C4	Cancer tissues	55	26 (47.27%)	29 (52.73%)	0.126
	Adjacent tissues	55	34 (61.82%)	21 (38.18%)	

Note: Difference in staining between cancer and adjacent tissues was considered as significant with $P < 0.05$.

Table 2 Correlation analysis of human AKRs with HCC differentiation degree

AKR	Staining	Total No.	Tumor differentiation degree			*P* value
			Low	Medium	Well	
AKR1A1	Negative					0.166
		37	13	13	11	
	Positive					
		18	8	2	8	
AKR1B10	Negative					0.037
		18	11	2	5	
	Positive					
		37	10	13	14	
AKR1C1/1C2	Negative					0.121
		36	16	11	9	
	Positive					
		19	5	4	10	
AKR1C3	Negative					0.381
		22	7	5	10	
	Positive					
		33	14	10	9	
AKR1C4	Negative					0.456
		26	8	7	11	
	Positive					
		29	13	8	8	

Note: Correlation was considered as significant with $P < 0.05$.

worthwhile question for later investigation. Furthermore, overexpression of AKR1B10 at both mRNA and protein levels in HuH7 raised two questions as to why the signals for transcript and protein expression were so strong for AKR1B10 and what would be associated with such overexpression. Abundance distribution of AKR1A1, AKR1B1 and AKR1B10 was similar in the hepatic cell lines examined except for HuH7. On the other hand, AKR7A2 expression exhibited some cell-type dependence. For instance, abundance of AKR7A2 in SMMC7721 was much higher than that in the other cell lines. The distribution of the AKR1C protein abundance was correlated with the cell lines as well. Relative abundance of AR1C1/1C2 to AKR1C3 showed different patterns in L-02, HepG2, HuH7 and SMMC7721. The protein abundance of AKR1C4 in L-02 was obviously lower than that in the tumor cell lines, which is similar to the observation in the AKR1C4 mRNA abundance. Therefore, if HuH7 is not considered, the quantitative proteomics results support the conclusion that the abundance distribution of AKR1A and AKR1B demonstrates the similar pattern in L-02, HepG2, BEL7402 and SMMC7721, while abundance of AKR1C displays a tumor-associated pattern.

Evaluation of the AKR protein expression status in hepatic tissues

To specifically examine the expression of respective AKR proteins, we expressed and purified 14 recombinant AKR proteins (in full or partial sequences), which were used as antigens to generate antibodies against various AKRs. In total, five specific monoclonal AKR antibodies that were prepared in our laboratory, including AKR1A1 S65, AKR1B10 S2, AKR1C1/1C2 S29, AKR1C3 S8 and AKR1C4 S34, were shown to be successful as IHC antibodies. We collected 55 HCC samples and 55 adjacent tissue (non-HCC) samples, which included 19 pairs of well-differentiated tissues, 15 pairs of medium-differentiated ones and 21 pairs of low-differentiated ones in the tissue samples, from HCC patients, each consisting of an HCC tumor samples and adjacent tissue samples. IHC was performed for these samples using the aforementioned AKR antibodies. Our results demonstrated varied staining pattern in tissues with different AKR antibodies (**Figure 3**). Analysis of the 55 HCC and 55 non-HCC samples revealed that positive staining for AKR1A1 appeared in 32.7% of the HCC samples (18 samples) examined and 58.2% of the non-HCC samples (32 samples) (**Table 1**). Similarly, we showed that AKR1B10 was detected in 67.3% (37 samples) of the tumor tissues and 41.8% of the non-HCC samples (23 samples). Further statistical analysis indicated that differences in IHC signals for AKR1A1 and AKR1B10 between the tumor and adjacent tissues were significant in these paired samples ($P < 0.05$, Table 1), while no significant difference was observed for AKR1C proteins ($P > 0.05$, Table 1). We then went further to detect whether the staining for AKR proteins was associated with the differentiation states of HCC. Our analysis showed that no significant correlation was found for staining of AKR1A1 and AKR1C1–1C4 proteins and the differentiation stages ($P > 0.05$, **Table 2**). However, the heavy staining of AKR1B10 was significantly associated with the differentiation states of HCC, due to the presence of the significant correlation ($P = 0.037$, Table 2).

Although the controversial results obtained from the AKR measurements in cells and tissues were somewhat disappointing, the data are still worthy of further investigation. First of all, AKRs are important detoxification enzymes in the liver and the relatively high abundances of AKRs are expected in the normal liver. IHC data in the adjacent tissues are

consistent with their important roles under normal conditions. Thus, the high background expression of AKRs may set the obstacle to distinguishing small differences in AKRs between tumor and adjacent tissues with IHC. Secondly, the sample collection may be another source of experimental errors. How to get samples with a high percentage of tumor cells is always challenging. Thirdly, AKRs are expressed in many tissues, including connective tissue and vessels [37]. AKR detection in a relatively pure cell population (such as a cell line) is likely different from a mixed cell population (excised tissues).

Discussion

The technical obstacles in quantitative evaluation of AKR expression status were priority considerations when we initiated this project. There are fewer technical challenges for quantitative measurement of AKR transcripts, since PCR products corresponding to the individual AKRs were satisfactorily amplified with properly-designed primers and appropriate PCR conditions for quantification. In order to globally estimate AKR protein abundances, our laboratory has developed an approach based upon antibody recognition [38]. Using Pan-AKR-P4, an antibody generated in our lab with high affinity to all the mouse AKR proteins, for 2-DE immunoblotting to examine the AKR abundances in mouse liver and kidney, our semi-quantitative data were in good agreement with other previous reports [39]. This technique is useful to evaluate the sum abundance of AKRs, nevertheless, it is useless for globally evaluating and comparing abundance of individual AKRs. Importantly, antibody-based measurement of AKRs offers relative limited information in accurate quantification. In this study, we utilized the mTRAQ/MRM approach to quantitatively measure the absolute abundances of the individual AKRs in hepatic cell lines. MRM measurement of AKRs in these hepatic cell lines provided relatively accurate data in protein quantification with the acceptable coefficient of variation values (Figure 2). The absolute quantification of AKRs thus makes it possible to globally and quantitatively evaluate contribution of various AKRs to different cancer cell lines. Taken together, both quantitative techniques were established to evaluate AKR expression status. Importantly, such strategy of quantitative evaluation can be potentially applied to other protein families.

The quantitative data in this study revealed that the AKR1C members are likely to be associated with hepatic tumor because abundance patterns of AKRs at either mRNA or protein levels were quite diverse among the cell lines examined. On the other hand, AKR1A and AKR1B appear to have a relatively stable abundance in these cell lines. Functional plasticity of AKR1Cs highlights their ability to modulate the levels of active hormones such as androgens, oestrogens and progestins [25,40–42]. For instance, 20-alpha-hydroxysteroid is an AKR1C1 substrate, while 3-alpha- and 17-beta-hydroxysteroid are oxidized by AKR1C2, AKR1C3 and AKR1C4 [43]. Hormone-dependent tissues require local production of androgens and estrogens to stimulate cell proliferation [25]. Penning et al. proposed that participation of AKR1Cs in conversion of hormones and their derivatives may stimulate the growth of hormone-dependent and -independent prostate and breast cancer [25,44,45]. In addition, some investigators found that the AKR1Cs were correlated with hormone-independent malignancies [20,46]. Figueroa et al. reported that overexpression of AKR1C3 was a high-risk factor in bladder cancer [47], while Hsu et al. observed that AKR1C mRNAs were not detected in the normal lung tissues but were overexpressed in 47% of the patients with non-small cell lung cancer (NSCLC) [18]. Although many documents indicate that AKR1C proteins play some roles in tumorigenesis, involvement of AKR1C in liver cancer is still a new view in the field. There is lack of evidence in the literature to support this hypothesis. IHC data generated from this study unfortunately did not provide supportive evidence to this hypothesis, due to the contradictory results with MRM data. More experiments are necessary to solve this caveat, since the quantitative data were generated upon solid experimental bases, and cross validated at mRNA and protein levels in cell lines, we could not find any reason to doubt about their accuracy. One option is to conduct the parallel experiments to test the AKR expression status in the liver cells both *in vitro* and *in vivo*.

Laffin and Petrash examined expression of AKR1B1 and AKR1B10 across all major human cancer types using database searching [48,49]. They found that AKR1B10 was significantly overexpressed in cancers of lung and liver, while AKR1B1 was more broadly overexpressed in human cancers but with a generally lower magnitude. Abnormal expression of AKRlB10 was also detected in HuH7 cells and most HCC tissues. A somewhat surprising result came from the quantitative data for AKR1B10 mRNA and protein in other cancer cell lines. In contrast to extremely high abundance of AKR1B10 mRNA and protein in HuH7 cells, three other liver cancer lines, HepG2, BEL7402 and SMMC7721, possessed almost normal levels of AKR1B10 mRNA and protein. More impressively, HuH7 cells showed global overexpression for most AKR genes, indicating that AKR1B10 overexpression is not a unique feature of tumorigenesis. Our data in quantitative mRNA and protein of AKR1B10 therefore prompt two questions. Is the HuH7 cell line more representative for liver cancer than other cancer cell lines? Is the AKR1B10 protein more stable in tissues or cells than other AKR members? No matter what the answer would be, the use of AKR1B10 for diagnosis and prognosis is of great potential interest and merits further investigation in the future.

Table 3 Features of the five hepatic cell lines examined in this study

Cell line	Origin	Ethnicity/race	Age (years)	Gender	Differentiation degree	Morphology
L-02	Liver	Chinese	–	–	Immortalized	Epithelial
HepG2	HCC	Caucasian	15	Male	Well-medium differentiated	Epithelial
HuH7	HCC	Japanese	57	Male	Well differentiated	Epithelial
SMMC7721	HCC	Chinese	50	Male	Medium–low differentiated	Epithelial
BEL7402	HCC	Chinese	53	Male	Medium–low differentiated	Epithelial

Materials and methods

Cell lines and tissues

L-02, BEL7402 and SMMC7721 cells were cultured in RPMI 1640 medium plus 10% FBS at 37 °C with 5% CO_2. HepG2 and HuH7 cells were cultured in DMEM medium plus 10% FBS at 37 °C with 5% CO_2. L-02 is a relatively normal hepatic cell line, while the others are HCC cell lines characterized by various degrees of differentiation. HepG2 and HuH7 are well-medium differentiated cell lines, while BEL7402 and SMMC7721 are medium–low differentiated cell lines (**Table 3**).

Thirty two paired hepatic tissues of patients consisting of the HCC portions with their corresponding adjacent tissues and 10 unpaired ones were obtained from the Department of Oncology, General Hospital of PLA. And 13 pairs of tissues were gifts from Xiaohang Zhao's lab in Cancer Institute and Cancer Hospital, Chinese Academy of Medical Sciences and Peking Union Medical College. Among them, 19 are well-differentiated ones, 15 are medium-differentiated ones and 21 are low-differentiated ones. The study was approved by the Research Ethics Boards of General Hospital of PLA and Cancer Institute and Cancer Hospital, Chinese Academy of Medical Sciences and Peking Union Medical College. Informed consent forms were obtained from all patients.

Quantitative real-time PCR analysis

Total RNAs were extracted from the five hepatic cell lines with TRIzol reagent (Invitrogen, Carlsbad, CA, USA) and reversely transcribed to generate cDNA libraries using reverse transcriptase M-MLV (Promega, Madison, WI, USA). Primers specific for respective AKR genes were designed using PrimerQuest software (IDT DNA, Coralville, IA, USA) and sequences of primers were listed in Table S2. Transcript levels of AKRs in the aforementioned hepatic cell lines were quantitatively evaluated using real-time PCR with an ABI PRISM 7300 Sequence Detection System (Applied Biosystems, Foster City, CA, USA) and EvaGreen dye (OPE Tech, Shanghai, China). The first step of cycling was 5 min at 95 °C followed by 40 cycles of 95 °C for 15 s, 60 °C for 15 s, 72 °C for 15 s and 80 °C for 30 s, then 10 min at 72 °C. The second step is dissociation stage, 95 °C for 15 s, 60 °C for 15 s and 95 °C for 15 s. Triplicate cDNA template samples were amplified and analyzed. All samples were tested three times. Identity of all the real-time PCR products was verified by sequencing (Figure S1).

Cell harvest and protein extraction

The hepatic cells were harvested by trypsin treatment. After rinsed with saline solution, cells were incubated with lysis buffer containing 8 M urea, 4% CHAPS, 10 mM DTT, 1 mM PMSF, 1 mM EDTA and 40 mM Tris–HCl (pH 8.5). After centrifugation at 20,000*g* for 20 min at 4 °C, the supernatant was removed and used as protein sample for electrophoresis on 12% SDS–PAGE gels.

Quantitative MRM analysis

Protein levels of AKRs in hepatic cell lines were quantified by MRM with QTRP 5500 (Applied Biosystems, Foster City, CA, USA) and unique peptides. MRM pilot software (Applied Biosystems) was used to design transitions of unique peptides. The sequences of unique peptides and corresponding transitions are listed in Table S1. We excised the bands at 34–42 KDa (about molecular weight of AKRs) to reduce the complexity of the samples. These samples were processed for trypsin digestion, mTRAQ label and MRM analysis.

Antigen expression

PCR products were verified by sequencing analysis. To produce the recombinant proteins, AKR1C1–1C4 were ligated into pET30a(+) vectors, while the others were ligated into pET28a(+), all fused in frame with N-terminal 6× His. Plasmids containing respective AKR1 sequences were transformed into *Escherichia coli* BL21(DE3) for protein expression. All the recombinant proteins were produced and purified with the Ni-NTA spin column as instructed by manufacturer (Qiagen, Venlo, Netherlands), which were used as antigens in full length or truncated fragments for antibody generation.

Generation and selection of monoclonal antibodies

BALB/c mice were used for immunization of the AKR recombinant proteins. After four times of immunization, the splenocytes were isolated and fused with a hypoxanthin–aminopterin–thymidine (HAT)-sensitive mouse myeloma cell line, SP2/0-Ag14, using polyethylene glycol method [50]. Hybridomas producing specific monoclonal antibody to AKRs were selected, amplified and then injected into enterocoelia of mice. Monoclonal antibody purification was carried out by affinity chromatography method. Antibodies of IgG subclass were purified on Protein G beads while antibodies of IgM and IgA subclasses were purified on Protein L beads [50].

ELISA experiments were designed to select the specific monoclonal antibodies of AKRs (BPI, Beijing, China) to avoid cross reaction between AKR members. Each well was coated with 10 ng AKR recombinant proteins. Specific antibodies should only recognize the corresponding antigen without any signal from the other AKRs.

Immunoblotting

Dot blotting analysis was performed to validate specificities and sensitivities of the respective monoclonal antibodies (Figure S2A). Protein concentration was determined by the Bradford method (Bio-Rad, Hercules, CA, USA). Recombinant AKR proteins were dotted on PVDF membranes (Millipore, Billerica, MA, USA) with increasing amounts (1, 10, 100 and 1000 ng). Membranes were then blocked in 5% milk in 1× Tris-buffered saline Tween (TBST) overnight at 4 °C and incubated with a specific primary antibody (listed below) in 5% milk for 1 h at 37 °C. Blots were washed in 1× TBST three times before incubated with an anti mouse secondary antibody conjugated with HRP (ZB2305, ZSGB-BIO, Beijing, China) for 1 h at room temperature. Finally, blots were washed and bands were visualized by the Image Quant ECL equipment (GE healthcare, Piscataway, NJ, USA). Primary antibodies against AKRs and the working concentrations are as follows: AKR1A1 S65 (1:700); AKR1B1 S1 (1:700); AKR1B10 S2 (1:8000); AKR1C1/1C2 S29 (1:10,000); AKR1C3 S8 (1:7000); AKR1C4 S34 (1:1000) and AKR7A2 S3 (1:1000).

In addition, specificities of the monoclonal antibodies were also validated with Huh7 cell lysate following the standard protocols using the aforementioned antibodies (Figure S2B).

IHC

The protein levels of AKRs in the HCC samples and adjacent tissues from patients were examined using IHC. Briefly, tissue sections were mounted and baked at 65 °C for 1–2 h. Sections were deparaffinized with xylene and re-hydrated in graded ethanol. Antigen retrieval was performed with 10 mM sodium citric acid buffer (pH 6.0) at high pressure for 2.5 min. Endogenous peroxidase activity was blocked by incubating the tissue sections with 3% H_2O_2 for 15 min. Antibodies were diluted with the blocking buffer and incubation in a moist chamber at 4 °C overnight. After washing, the slides were treated with ready to use secondary antibody (ZB2305) and incubated at 37 °C for 25 min, followed by rinses with PBS. DAB substrate was added to the slides and incubated at room temperature for less than 10 min. Tissue sections were counterstained lightly with hematoxylin. Slides were dehydrated and sealed with neutral balsam for visualization by light microscopy. Primary antibodies against AKRs and the working concentrations are as follows: AKR1A1 S65 (1:500); AKR1B10 S2 (1:10,000); AKR1C1/1C2 S29 (1:10,000); AKR1C3 S8 (1:5000) and AKR1C4 S34 (1:200). The staining was scored as negative (if $<5\%$ cells were stained in a field examined) or positive (if $\geqslant 5\%$ cells were stained in a field examined) by pathologists and research scientists independently.

Statistical analysis

Results are presented as the mean ± standard error. Statistical significance was set at $P < 0.05$. For real-time PCR, the Ct values of housekeeping gene *β-actin* were adopted to normalize the expression of AKRs. The comparison of mRNA levels between the cell lines was achieved on the basis of the relative values of gene expression calculated by $2^{\triangle\triangle Ct}$ method [51]. One-way ANOVA and 2-way ANOVA were used for statistical analysis. For MRM, *t* test was used to determine *P* values between samples. And for IHC, statistical analysis was carried out by Pearson χ^2 test.

Authors' contributions

LY performed most of the experiments. JZ was involved in data analysis. SZ constructed the recombinant plasmids of AKR1C members and carried out the MRM experiments. WD supplied 42 pairs of HCC and their adjacent tissues. XL and SL participated in study design and coordination. LY drafted the manuscript with the help of XL and SL. All authors read and approved the final manuscript.

Competing interests

The authors have declared no competing interests.

Acknowledgements

This study was supported by the National High-tech R&D Program of China (Grant No. 2012AA020206). Some AKR cDNAs are gifts from Jiahuai Han's lab, School of Life Sciences, Xiamen University. We thank Qin Su (Department of Pathology, Cancer Institute and Cancer Hospital, Chinese Academy of Medical Sciences and Peking Union Medical College) and Bin Dong (Department of Pathology, Peking University Cancer Hospital/Institute) for reading IHC slides.

Supplementary material

Supplementary material associated with this article can be found, in the online version, at http://dx.doi.org/10.1016/j.gpb.2013.04.001.

References

[1] Bohren KM, Bullock B, Wermuth B, Gabbay KH. The aldo–keto reductase superfamily. cDNAs and deduced amino acid sequences of human aldehyde and aldose reductases. J Biol Chem 1989;264:9547–51.
[2] Seery LT, Nestor PV, FitzGerald GA. Molecular evolution of the aldo–keto reductase gene superfamily. J Mol Evol 1998;46:139–46.
[3] Jez JM, Penning TM. The aldo–keto reductase (AKR) superfamily: an update. Chem Biol Interact 2001;130–132:499–525.
[4] Jin Y, Penning TM. Aldo–keto reductases and bioactivation/detoxication. Annu Rev Pharmacol Toxicol 2007;47:263–92.
[5] Penning TM, Drury JE. Human aldo–keto reductases: function, gene regulation, and single nucleotide polymorphisms. Arch Biochem Biophys 2007;464:241–50.
[6] Ruiz FX, Porte S, Pares X, Farres J. Biological role of aldo–keto reductases in retinoic acid biosynthesis and signaling. Front Pharmacol 2012;3:58.
[7] Knight LP, Primiano T, Groopman JD, Kensler TW, Sutter TR. CDNA cloning, expression and activity of a second human aflatoxin B1-metabolizing member of the aldo–keto reductase superfamily, AKR7A3. Carcinogenesis 1999;20:1215–23.
[8] Penning TM. AKR1B10: a new diagnostic marker of non-small cell lung carcinoma in smokers. Clin Cancer Res 2005;11:1687–90.
[9] Fukumoto S, Yamauchi N, Moriguchi H, Hippo Y, Watanabe A, Shibahara J, et al. Overexpression of the aldo–keto reductase family protein AKR1B10 is highly correlated with smokers' non-small cell lung carcinomas. Clin Cancer Res 2005;11:1776–85.
[10] Li CP, Goto A, Watanabe A, Murata K, Ota S, Niki T, et al. AKR1B10 in usual interstitial pneumonia: expression in squamous metaplasia in association with smoking and lung cancer. Pathol Res Pract 2008;204:295–304.
[11] Kang MW, Lee ES, Yoon SY, Jo J, Lee J, Kim HK, et al. AKR1B10 is associated with smoking and smoking-related non-small-cell lung cancer. J Int Med Res 2011;39:78–85.
[12] Cardarella S, Ortiz TM, Joshi VA, Butaney M, Jackman DM, Kwiatkowski DJ, et al. The introduction of systematic genomic testing for patients with non-small-cell lung cancer. J Thorac Oncol 2012;7:1767–74.
[13] Lin HK, Steckelbroeck S, Fung KM, Jones AN, Penning TM. Characterization of a monoclonal antibody for human aldo–keto reductase AKR1C3 (type 2 3alpha-hydroxysteroid dehydrogenase/type 5 17beta-hydroxysteroid dehydrogenase); immunohistochemical detection in breast and prostate. Steroids 2004;69:795–801.
[14] Ji Q, Aoyama C, Nien YD, Liu PI, Chen PK, Chang L, et al. Selective loss of AKR1C1 and AKR1C2 in breast cancer and their

potential effect on progesterone signaling. Cancer Res 2004;64: 7610–7.
[15] Lan Q, Zheng T, Shen M, Zhang Y, Wang SS, Zahm SH, et al. Genetic polymorphisms in the oxidative stress pathway and susceptibility to non-Hodgkin lymphoma. Hum Genet 2007;121: 161–8.
[16] Saraswat M, Mrudula T, Kumar PU, Suneetha A, Rao Rao TS, Srinivasulu M, et al. Overexpression of aldose reductase in human cancer tissues. Med Sci Monit 2006;12:CR525–9.
[17] Saxena A, Tammali R, Ramana KV, Srivastava SK. Aldose reductase inhibition prevents colon cancer growth by restoring phosphatase and tensin homolog through modulation of miR-21 and FOXO3a. Antioxid Redox Signal 2013;18:1249–62.
[18] Hsu NY, Ho HC, Chow KC, Lin TY, Shih CS, Wang LS, et al. Overexpression of dihydrodiol dehydrogenase as a prognostic marker of non-small cell lung cancer. Cancer Res 2001;61: 2727–31.
[19] Palackal NT, Lee SH, Harvey RG, Blair IA, Penning TM. Activation of polycyclic aromatic hydrocarbon trans-dihydrodiol proximate carcinogens by human aldo–keto reductase (AKR1C) enzymes and their functional overexpression in human lung carcinoma (A549) cells. J Biol Chem 2002;277:24799–808.
[20] Nagaraj NS, Beckers S, Mensah JK, Waigel S, Vigneswaran N, Zacharias W. Cigarette smoke condensate induces cytochromes P450 and aldo–keto reductases in oral cancer cells. Toxicol Lett 2006;165:182–94.
[21] Lister A, Nedjadi T, Kitteringham NR, Campbell F, Costello E, Lloyd B, et al. Nrf2 is overexpressed in pancreatic cancer: implications for cell proliferation and therapy. Mol Cancer 2011;10:37.
[22] Wang LS, Chow KC, Wu YC, Lin TY, Li WY. Inverse expression of dihydrodiol dehydrogenase and glutathione-S-transferase in patients with esophageal squamous cell carcinoma. Int J Cancer 2004;111:246–51.
[23] Chang HC, Chen YL, Chan CP, Yeh KT, Kuo SJ, Ko CJ, et al. Overexpression of dihydrodiol dehydrogenase as a prognostic marker in resected gastric cancer patients. Dig Dis Sci 2009;54:342–7.
[24] Nomura M, Fukuda T, Fujii K, Kawamura T, Tojo H, Kihara M, et al. Preferential expression of potential markers for cancer stem cells in large cell neuroendocrine carcinoma of the lung. An FFPE proteomic study. J Clin Bioinform 2011;1:23.
[25] Penning TM, Byrns MC. Steroid hormone transforming aldo–keto reductases and cancer. Ann NY Acad Sci 2009;1155:33–42.
[26] Tai HL, Lin TS, Huang HH, Lin TY, Chou MC, Chiou SH, et al. Overexpression of aldo–keto reductase 1C2 as a high-risk factor in bladder cancer. Oncol Rep 2007;17:305–11.
[27] Huang KH, Chiou SH, Chow KC, Lin TY, Chang HW, Chiang IP, et al. Overexpression of aldo–keto reductase 1C2 is associated with disease progression in patients with prostatic cancer. Histopathology 2010;57:384–94.
[28] Quinn AM, Penning TM. Comparisons of (+/−)-benzo[a]pyrene-trans-7,8-dihydrodiol activation by human cytochrome P450 and aldo–keto reductase enzymes: effect of redox state and expression levels. Chem Res Toxicol 2008;21:1086–94.
[29] Lord SJ, Mack WJ, Van Den Berg D, Pike MC, Ingles SA, Haiman CA, et al. Polymorphisms in genes involved in estrogen and progesterone metabolism and mammographic density changes in women randomized to postmenopausal hormone therapy: results from a pilot study. Breast Cancer Res 2005;7: R336–44.
[30] Jez JM, Bennett MJ, Schlegel BP, Lewis M, Penning TM. Comparative anatomy of the aldo–keto reductase superfamily. Biochem J 1997;326(Pt 3):625–36.
[31] Chang Q, Petrash JM. Disruption of aldo–keto reductase genes leads to elevated markers of oxidative stress and inositol auxotrophy in *Saccharomyces cerevisiae*. Biochim Biophys Acta 2008;1783:237–45.
[32] Ho HT, Chung SK, Law JW, Ko BC, Tam SC, Brooks HL, et al. Aldose reductase-deficient mice develop nephrogenic diabetes insipidus. Mol Cell Biol 2000;20:5840–6.
[33] Zeindl-Eberhart E, Jungblut PR, Otto A, Rabes HM. Identification of tumor-associated protein variants during rat hepatocarcinogenesis aldose reductase. J Biol Chem 1994;269:14589–94.
[34] Takahashi M, Fujii J, Miyoshi E, Hoshi A, Taniguchi N. Elevation of aldose reductase gene expression in rat primary hepatoma and hepatoma cell lines: implication in detoxification of cytotoxic aldehydes. Int J Cancer 1995;62:749–54.
[35] Cao D, Fan ST, Chung SS. Identification and characterization of a novel human aldose reductase-like gene. J Biol Chem 1998;273: 11429–35.
[36] Goh WW, Lee YH, Ramdzan ZM, Sergot MJ, Chung M, Wong L. Proteomics signature profiling (PSP): a novel contextualization approach for cancer proteomics. J Proteome Res 2012;11: 1571–81.
[37] Reddy AB, Ramana KV. Aldose reductase inhibition: emerging drug target for the treatment of cardiovascular complications. Recent Pat Cardiovasc Drug Discov 2010;5:25–32.
[38] Tu S, Ren Y, Tong W, Zheng S, Xu N, Bhatnagar A, et al. A new approach to monitor expression of aldo–keto reductase proteins in mouse tissues. Proteomics 2009;9:5090–100.
[39] Vergnes L, Phan J, Stolz A, Reue K. A cluster of 8 hydroxysteroid dehydrogenase genes belonging to the aldo–keto reductase supergene family on mouse chromosome 13. J Lipid Res 2003;44: 503–11.
[40] Rizner TL, Smuc T, Rupreht R, Sinkovec J, Penning TM. AKR1C1 and AKR1C3 may determine progesterone and estrogen ratios in endometrial cancer. Mol Cell Endocrinol 2006;248: 126–35.
[41] Fung KM, Samara EN, Wong C, Metwalli A, Krlin R, Bane B, et al. Increased expression of type 2 3alpha-hydroxysteroid dehydrogenase/type 5 17beta-hydroxysteroid dehydrogenase (AKR1C3) and its relationship with androgen receptor in prostate carcinoma. Endocr Relat Cancer 2006;13:169–80.
[42] Bauman DR, Steckelbroeck S, Penning TM. The roles of aldo–keto reductases in steroid hormone action. Drug News Perspect 2004;17:563–78.
[43] Penning TM, Jin Y, Steckelbroeck S, Lanisnik Rizner T, Lewis M. Structure-function of human 3 alpha-hydroxysteroid dehydrogenases: genes and proteins. Mol Cell Endocrinol 2004;215: 63–72.
[44] Penning TM, Burczynski ME, Jez JM, Hung CF, Lin HK, Ma H, et al. Human 3alpha-hydroxysteroid dehydrogenase isoforms (AKR1C1–AKR1C4) of the aldo–keto reductase superfamily: functional plasticity and tissue distribution reveals roles in the inactivation and formation of male and female sex hormones. Biochem J 2000;351:67–77.
[45] Penning TM, Steckelbroeck S, Bauman DR, Miller MW, Jin Y, Peehl DM, et al. Aldo–keto reductase (AKR) 1C3: role in prostate disease and the development of specific inhibitors. Mol Cell Endocrinol 2006;248:182–91.
[46] Miller VL, Lin HK, Murugan P, Fan M, Penning TM, Brame LS, et al. Aldo–keto reductase family 1 member C3 (AKR1C3) is expressed in adenocarcinoma and squamous cell carcinoma but not small cell carcinoma. Int J Clin Exp Pathol 2012;5:278–89.
[47] Figueroa JD, Malats N, Garcia-Closas M, Real FX, Silverman D, Kogevinas M, et al. Bladder cancer risk and genetic variation in AKR1C3 and other metabolizing genes. Carcinogenesis 2008;29: 1955–62.
[48] Laffin B, Petrash JM. Expression of the aldo–keto reductases AKR1B1 and AKR1B10 in Human Cancers. Front Pharmacol 2012;3:104.

[49] Petrash JM, Murthy BS, Young M, Morris K, Rikimaru L, Griest TA, et al. Functional genomic studies of aldo–keto reductases. Chem Biol Interact 2001;130–132:673–83.
[50] Lim HH, Fang Y, Williams C. High-efficiency screening of monoclonal antibodies for membrane protein crystallography. PLoS One 2011;6:e24653.
[51] Zhang J, Kang B, Tan X, Bai Z, Liang Y, Xing R, et al. Comparative analysis of the protein profiles from primary gastric tumors and their adjacent regions: MAWBP could be a new protein candidate involved in gastric cancer. J Proteome Res 2007; 6:4423–32.